Korean J. Chem. Eng., **27**(2), 705-715 (2010)
DOI: 10.1007/s11814-010-0104-z

Effect of added ionomer on morphology and properties of PP/organoclay nanocomposites

Hyung Tag Lim*, Hongzhe Liu*, Kyung Hyun Ahn*,†, Seung Jong Lee*, and Joung Sook Hong**

*School of Chemical and Biological Engineering, Seoul National University, Seoul 151-744, Korea
**Department of Chemical and Environmental Engineering, Soongsil University, Seoul 156-743, Korea
(*Received 1 July 2009 • accepted 12 November 2009*)

Abstract−Ethylene-methacrylic acid ionomer (Surlyn) with concentration up to 20 wt% based on total weight of polymer resin was added into polypropylene (PP)/organoclay hybrids. The microstructure, rheological properties, crystallization properties and mechanical properties of the obtained nanocomposites have been investigated. The addition of ionomer markedly enlarged interlayer spacing of the platelets and led to an improved degree of exfoliation. Moreover, clay silicates were found to selectively disperse either inside the ionomer phase or at the phase boundary. Compared to the binary immiscible blends, an improved interfacial adhesion was achieved for PP/Surlyn/OMMT hybrids. Unlike PP/Surlyn binary blends, the viscoelastic properties of the hybrids significantly increased with increasing Surlyn concentration, which could be attributed to the improved clay dispersion and the contribution of silicate layers at the interface between PP and Surlyn. A synergistic role between Surlyn and clay was also found to suppress the crystallization of PP matrix. In addition, PP/Surlyn/OMMT hybrids exhibited superior tensile strain compared to the corresponding PP/PP-g-MA/OMMT. Both tensile strength and elongation at break showed maximum at Surlyn concentration of 5 wt%. By comparing the experimental tensile yield strength with model prediction, it was suggested that the clay platelets localized at the interface could play a role of interfacial activation to some extent.

Key words: Nanocomposites, Poly(propylene) (PP), Clay, Ionomer, Surlyn, Morphology, Rheology

INTRODUCTION

Over the last few decades, a great amount of effort has been devoted to fabrication of polymer layered silicate nanocomposites because of their exceptionally improved mechanical properties, such as improved stiffness, barrier properties, and flame-retardance at low filler loading (3-5 wt%). The key to such an enhanced performance is widely believed to lie in the ability to exfoliate and disperse individual, high aspect ratio silicate platelets within the polymer matrix. Among the nanocomposites based on various polymers, polypropylene-clay nanocomposites (PPCN) have attracted special attention due to their commercial importance. However, unfortunately, it is still a great challenge to prepare PPCN with exfoliated structure. At present, the most widely recognized approach is to add maleic anhydride grafted PP (PP-g-MA) as a compatibilizer during melt intercalation.

As a class of ionomer, Surlyn® developed by Dupont is ethylene-co-methacrylic acid (E-MAA) polymer, in which a small amount of methyl-carboxylic acid is partially neutralized by metal bases, e.g., Na^+, Li^+ and Zn^{2+}. Here, the associated ionic groups form ion-rich domains in the nanometer size (ionic aggregates/cluster) in the hydrophobic polyethylene (PE) matrix. The presence of these aggregates deeply influences mechanical and melt-flow properties of the resulting materials. This ionomer exhibits superior abrasion resistance, transparency, scratch and scuff resistance, low temperature impact resistance, chemical resistance, melt strength, and adhesion properties to nonionic PE. The general molecular structure of Surlyn is as follows:

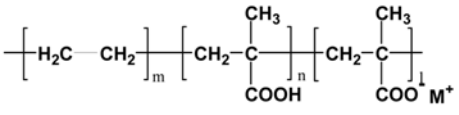

$M^+ = Na^+, Zn^{2+}, Li^+$

where m, n, and *l* are the segment number of units. The presence of the pendant ionic groups in the ionomer creates favorable interaction between ionomer and aluminosilicate clay. Several reports demonstrate that the addition of Surlyn remarkably improves exfoliation of clay platelets [1-4]. On the other hand, one of the major deficiencies of PPCN is low impact resistance, particularly at low temperature. This issue will be more serious for applications in which an optimum balance of stiffness and toughness is desired. There are some attempts to improve toughness of PPCN by adding elastomer [5-10].

The objective of this study is to investigate the effect of clay on interfacial properties of PP/Surlyn nanocomposites using X-ray diffraction, dynamic rheological measurement, scanning electron microscope, transmission electron microscopy, differential scanning calorimetry and tensile testing. Morphological analysis is related to rheological and thermal and mechanical properties.

EXPERIMENTAL

1. Materials

All the resins used are commercial products, among which the Surlyn was kindly provided by the DuPont Company. The charac-

†To whom correspondence should be addressed.
E-mail: ahnnet@snu.ac.kr
‡This paper is dedicated to Professor Jae Chun Hyun for celebrating his retirement from Department of Chemical and Biological Engineering of Korea University.

Table 1. Characteristics of materials used

Name	Trademark	Characteristics	Supplier
PP	HP562T	MFR (230 °C, 2.16 Kg)=6.0 g/min	Polymirae Company Ltd (Korea)
Ionomer	Surlyn®8945	MFR (190 °C, 2.16 Kg)=4.5 g/10 min, specific gravity=0.96, MAA%=15.2, [Na^+]%=1.99 wt%, neutralization=~40% [2]	DuPont company
OMMT	Cloisite®20A (i.e. Dimethyl bis(hydrogenated-tallow) ammonium montmorillonite)	CEC=95 meq/100 g, Organic content=39.6 wt%, specific gravity=1.77 [11]	Southern Clay Products

teristics of the above materials are summarized in Table 1. The content of OMMT is expressed in terms of parts per hundred total resins used (phr; including PP and Surlyn), and was kept at 5phr for all hybrids. Commercial PP-g-MA (Polybond®3200, MA%=1.0 by weight) was also added into PP/OMMT as a reference.

2. Blend Preparation

Prior to compounding, all the raw materials were dried in the vacuum oven at 80 °C for at least 12 hours. Melt compounding was performed using an intermeshing, co-rotating twin-screw extruder (diameter=19 mm, L/D=40; Bautek, Korea) at a screw speed of 100 rpm. The temperature of melting zone was set between 170 °C to 190 °C. As a reference, pure PP, Surlyn, and their binary blends were also extruded under the same condition. For morphology characterization, the pellets were compression-molded into disks with a diameter of 25 mm and a thickness of 1 mm using a hot press (Carver, CH4386) at 190 °C. For abbreviation, PP/Surlyn/OMMT and PP/Surlyn will be hereafter denoted as PPxCN and PPx, respectively, in which the number x means the concentration of the added Surlyn, while SurlynCN refers to the nanocomposite prepared from pure Surlyn.

3. Characterization

3-1. X-ray Diffraction

X-ray diffraction (XRD) was used to analyze the structure of layered silicates of composites on Rigaku D/MAX-IIIC X-ray diffractometer (Cu-Kα radiation, λ=1.5418) with accelerating voltage of 40 kV. Diffraction spectra were collected over a 2θ range of 1.2-10°.

3-2. Scanning Electron Microscope

The blend morphology was examined by Field-emission scanning electron microscope (FE-SEM) using a JEOL JSM-6700F apparatus operating at an accelerating voltage of 5 kV. The samples were fractured in liquid nitrogen and then sputter-coated with palladium to avoid charging during observation.

3-3. Transmission Electron Microscope

The dispersion of clay particles in polymer matrix was evaluated by high resolution transmission electron microscope (HR-TEM) using a JEOL JEM-3011 with an electron accelerating voltage of 300 kV. The TEM specimens were prepared by cryo-ultramicrotoming in the Korea Basic Science Institute.

3-4. Dynamic Rheological Measurement

The rheological properties were measured at 180 °C on RMS800 (Rheometrics Inc.) with a parallel plate fixture (25 mm diameter). To avoid thermal degradation of polymers, all measurements were performed under nitrogen atmosphere. The complex viscosity (η^*) and storage modulus (G') were recorded as a function of frequency (0.1-100 rad/s) using a dynamic oscillatory mode. Linear viscoelastic regime was determined by separate strain sweep test.

3-5. Tensile Testing

The specimens for tensile tests were prepared using HAAKE Minijet (Thermo Electron Corporation) in accordance with ASTM D638 type V. The barrel temperature was set at 180-190 °C. Prior to injection moulding, the extruded pellets were dried under vacuum at 80 °C overnight. Tensile samples were immediately placed into sealed polyethylene bag and stored in a vacuum desiccator before testing. Tensile tests were performed at room temperature according to ASTM D638 using Instron 1122 universal testing machine. The tensile properties were measured at a crosshead speed of 5.0 mm/min. At least five specimens for each sample were tested and average value was reported, together with its standard deviation.

3-6. Differential Scanning Calorimetry

Differential Scanning Calorimetry (DSC) measurement of the blends and their composites was performed using DSC 2010 (TA Instruments). Samples were first heated to 230 °C at a scanning rate of 10 °C/min and then maintained at this temperature for 5 min to erase previous thermal history before subsequent cooling at the same rate. All measurements were carried out in nitrogen atmosphere. The crystallinity of PP was determined using the following equation:

$$\chi = \frac{\Delta H_c}{f_p \Delta H_c^{100}} \times 100\% \quad (1)$$

where ΔH_c(J/g) is the measured enthalpy of crystallization of the sample, f_p is the PP weight fraction and ΔH_c^{100}(J/g) is a reference value that represents the enthalpy of crystallization for 100% crystalline polymer (209 J/g [12]).

RESULTS AND DISCUSSION

1. XRD

Fig. 1 shows a series of X-ray diffraction patterns (XRD) of original OMMT and its hybrids with varying concentration of Surlyn. Without Surlyn, the XRD pattern of PPCN fails to exhibit a significant increase (about 0.4 nm) in interlayer spacing (d_{001}) with respect to original Cloisite® 20A. In contrast, the effect of added Surlyn on magnitude of d_{001} is pronounced. When only 5 wt% Surlyn was added into PP/clay composites, the peak of the (001) basal diffraction of organoclay remarkably shifted to a lower angle. Interestingly, with further addition of Surlyn, the position of the characteristic peak almost remains unchanged.

At the concentration of 20 wt% ionomer, however, the d_{001} diffraction peak becomes more broadened and its intensity is weaker, whose pattern is similar to the silicate hybrid prepared by pure Surlyn.

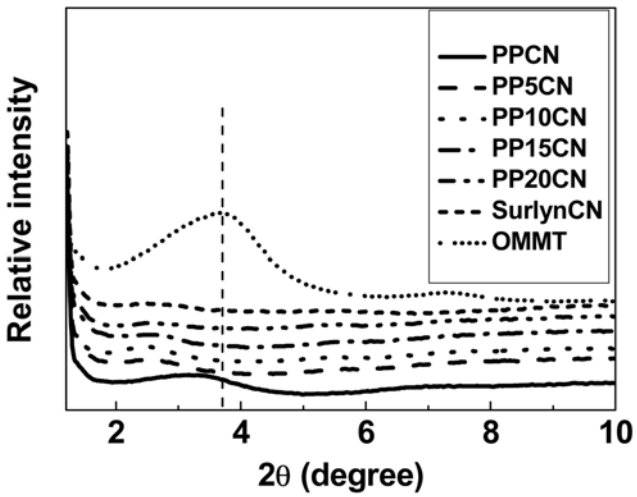

Fig. 1. XRD patterns for virgin OMMT and PP/PP-g-MA/OMMT with different OMMT contents.

As a result, the well-defined interlayer spacing is difficult to determine accurately. This result indicates that the stacks of layered silicates become more disordered, although a periodic distance is still maintained. Apparently, the partial exfoliation of the layered silicates could be responsible for the decrease in intensity.

2. Microscopic Observation

Fig. 2 shows SEM micrographs of cryo-fractured surfaces of PP/Surlyn binary blends. It is clearly observed that many smooth particles are debonding from PP matrix, suggesting poor interfacial adhesion between the phases. With increasing ionomer content, the size of the dispersed phase becomes larger, as is obviously observed above 10 wt%. The SEM pictures of PP/Surlyn/C20A composites are given in Fig. 3. In the case of uncompatibilized PP0CN, many clay tactoids are clearly observed (Fig. 3(a)), indicative of poor dispersion clays. However, a quite different situation occurs for PP/Surlyn/OMMT ternary hybrids. The perceptible clay tactoids are scarcely observed. This observation implies improved dispersion of clays in the polymer matrix upon the addition of the ionomer. In addition, the dispersed particles seem to be rarely discernible at the present magnification and the interfacial adhesion seems to be improved more or less. This observation is quite different from that of the above binary blends.

In order to further clarify the morphological details, TEM micrographs of PP/Surlyn/C20A nanocomposites with varying Surlyn concentration are given in Fig. 4. The addition of ionomer remarkably improves dispersion of clay tactoids. Moreover, exfoliation increases with concentration of added Surlyn. Above 15 wt% of the ionomer, clay layers consisting of 1-3 individual silicate platelets are clearly visible, suggesting that the exfoliation appears dominant in these hybrids as in SurlynCN (in Fig. 4(f)). In addition, it is interesting to note that these layers locate not only inside Surlyn domain but also at the phase boundary, but not in the PP matrix. To recall the improved interfacial adhesion indicated by the aforementioned SEM images, it is presumed that the clay platelets at the interface

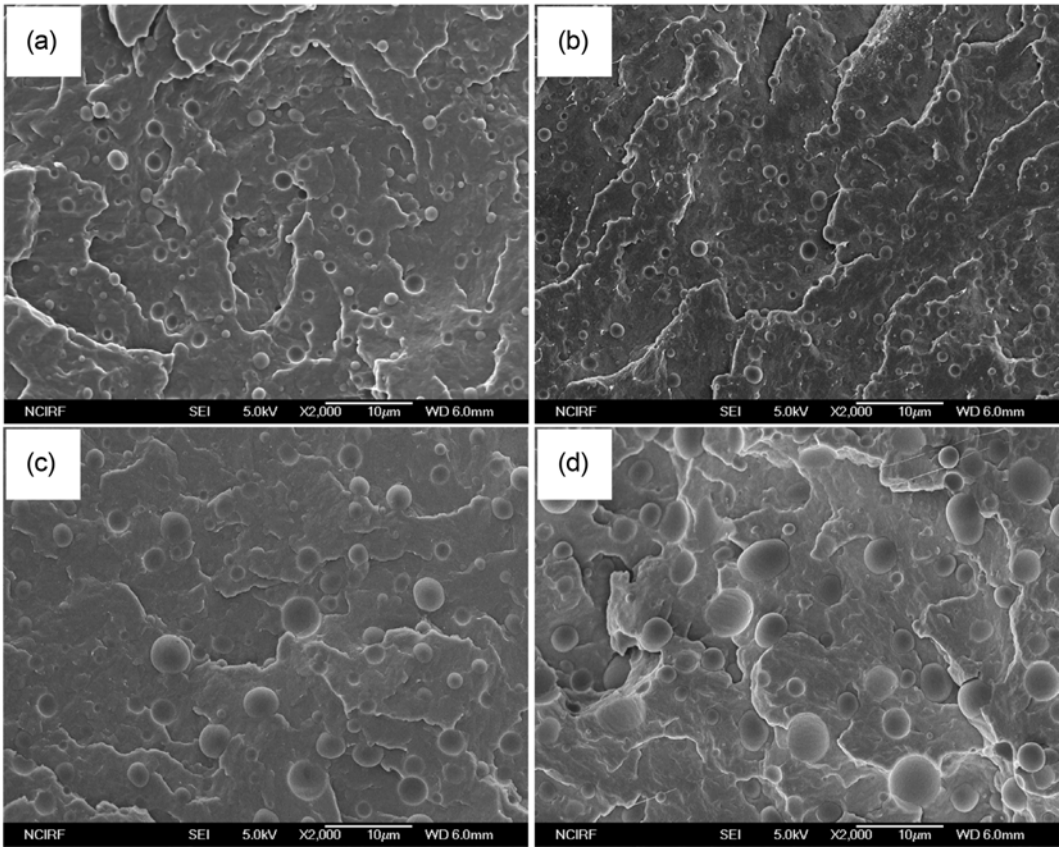

Fig. 2. Cryo-fractured SEM micrographs of PP/Surlyn blends: (a) 95/5; (b) 90/10; (c) 85/15; (d) 80/20.

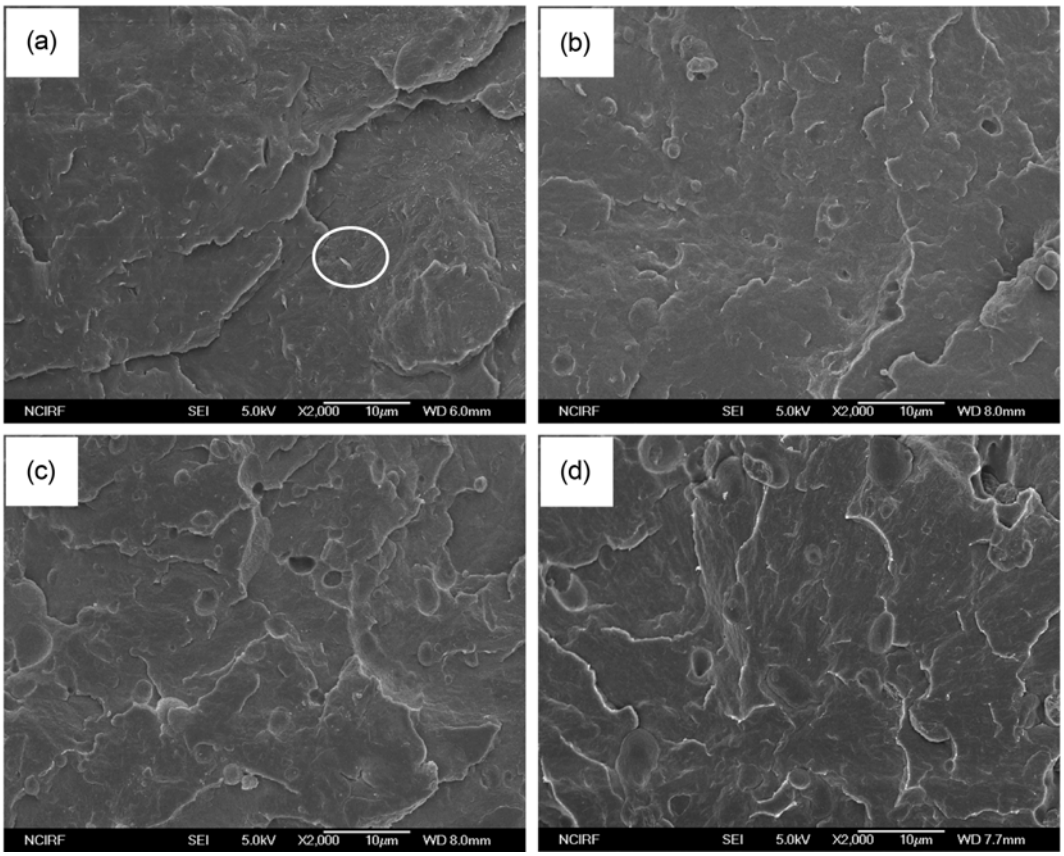

Fig. 3. Cryo-fractured SEM micrographs of PP/Surlyn/OMMT hybrids: (a) 100/0/5; (b) 95/5/5; (c) 90/10/5; (d) 85/15/5.

could play a role of interfacial activation in immiscible PP/Surlyn blends to some extent. Recently, selective localization of clay platelets at the interface of immiscible polymer blends was also reported [13-15]. Si et al. compared the morphology of many immiscible blends with and without commercial organoclays [13]. A large reduction in domain size and localization of the clay platelets along the interface was observed. In some cases, the increased miscibility was claimed on the basis of the reduction of multiple values of T_g to one. A model was proposed, in which in-situ grafts were formed on the clay surface during melt blending and consequently localized at the interface. Such an interfacial activity of OMMT localized at the interface was also observed by Ray and coworkers [14]. They reported that upon the addition of only 0.5 wt% C20A, the interfacial tension decreased from 5.1 to 3.4 mN/m for PS/PP and from 4.8 to 1.1 mN/m for PS/PP-g-MA blends. In addition, it was revealed that the viscosity ratio solely failed to explain the dramatic decrease in dispersed domain size. Hong et al. recently reported that the clay tactoids of the thickness of the order of 10 nm were heterogeneously distributed along the interface in PBT/PE blends [15]. They concluded that the presence of organoclay at the interface hydrodynamically stabilized the blend morphology by suppressing the coalescence of the droplets and also made the morphology thermally stable. The following results further corroborate such interfacial activation of OMMT.

3. Rheological Properties

Fig. 5 shows the storage modulus (G') and complex viscosity (η^*) as a function of frequency (ω) for PP/Surlyn blends, together with pure PP and Surlyn. The addition of ionomer results in a slight increase of both G' and η^* at low frequency on account of higher viscoelastic properties of Surlyn. In addition, the Newtonian plateau characteristic of pure PP remains unchanged as indicated in Fig. 5(b).

Dynamic rheological properties of PP/Surlyn/OMMT nanocomposites with varying concentration of Surlyn are given in Fig. 6. With increasing concentration of Surlyn, the storage modulus significantly increases especially at low frequency (about 2-3 orders of magnitude) with the leveling-off of terminal slope. At the concentration of 20 wt% Surlyn, the magnitude of G' is similar to that of SurlynCN, and even its non-terminal behavior at low frequency becomes more pronounced. Also, the complex viscosity exhibits the same tendency, and shear-thinning behavior becomes more pronounced at low frequency.

To isolate the effect of dispersion of the fillers, the relative viscosity (η^*_{rel}) has been defined as the magnitude of the complex viscosity of the composite divided by the complex viscosity of the silicate-free matrix (i.e., PP, PP/Surlyn, and Surlyn as the matrix of PP0CN, PP/Surly/OMMT and Surlyn, respectively). Fig. 7 presents the relative viscosity of the hybrids, in which a progressive enhancement in η^*_{rel} is observed especially at low frequency, as the content of the added ionomer increases. It implies that the clay dispersion becomes better with Surlyn concentration. Unexpectedly, the greatest enhancement of relative viscosity is observed for PP20CN rather than SurlynCN. This could be attributed to the increased interfacial contribution caused by the activation of silicate layers located between PP and Surlyn components as mentioned before. To further

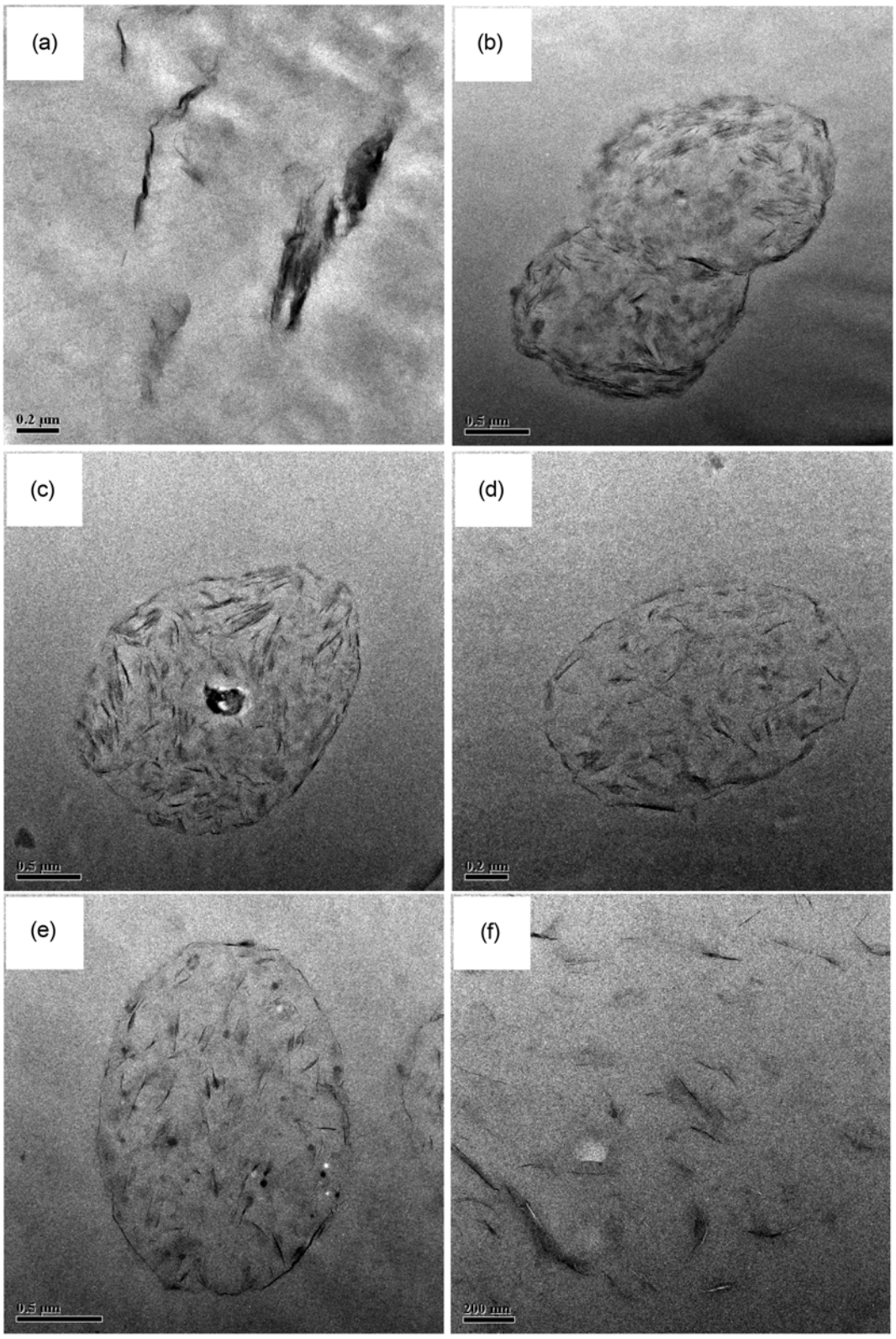

Fig. 4. TEM micrographs of PP/Surlyn/OMMT hybrids at high magnification: (a) 100/0/5; (b) 95/5/5; (c) 90/10/5; (d) 85/15/5; (e) 80/20/5; (f) 0/100/5.

verify whether the organoclay at the interface brings about the change in the dynamics at interface, additional rheological test was performed under oscillatory shear.

It is well known that the melt viscosity (η^*) of the blend depends not only on the contribution of each component but also on the interactions at the interface. With increasing interfacial adhesion, the

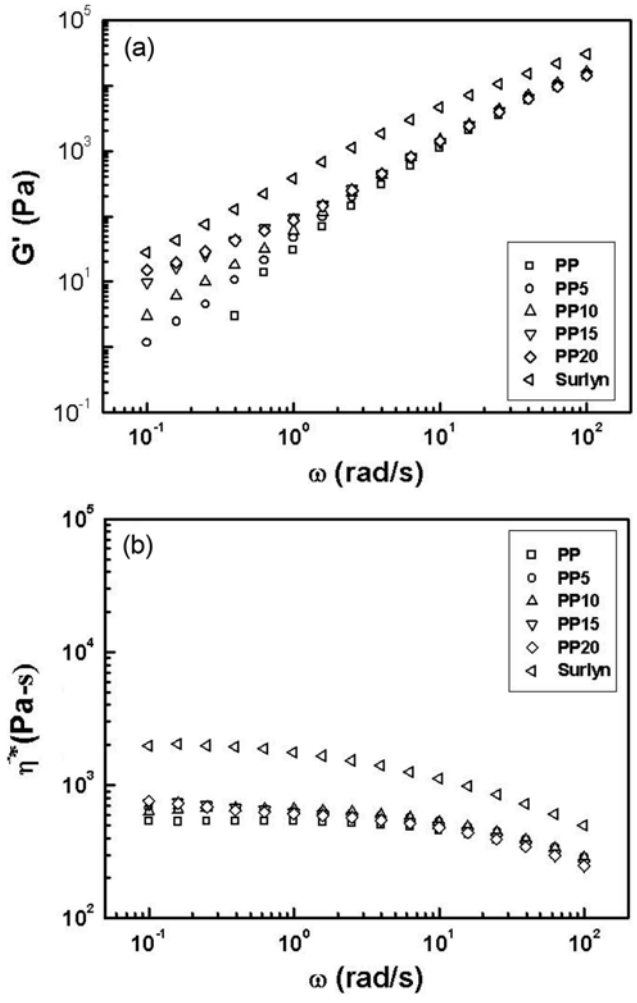

Fig. 5. Rheological data of PP/Surlyn blends at 180 °C: (a) storage modulus (G′); (b) complex viscosity (η^*).

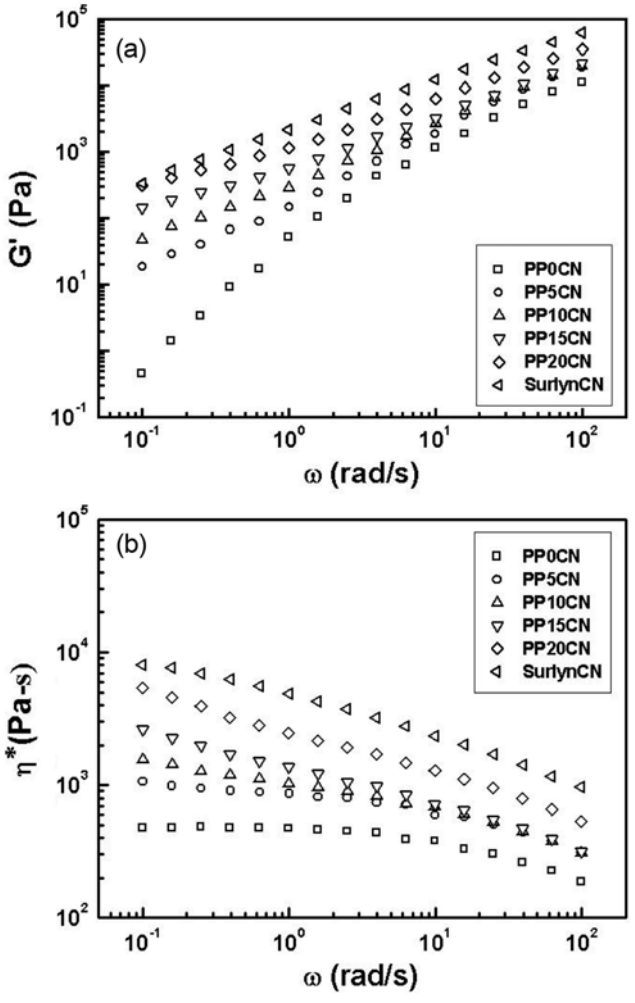

Fig. 6. Rheological data of PP/Surlyn/OMMT hybrids at 180 °C: (a) storage modulus (G′); (b) complex viscosity (η^*).

contribution from interface would be increased. For fully incompatible polymer blends, there exists no interfacial contribution due to poor adhesion between the components. Immiscible polymer blends with strong interfacial interaction often exhibit a positive deviation from the log-additivity rule, whereas the opposite effect is observed when the interaction is weak [17]. In our case, the clay layers locate only inside of the Surlyn domain and thus the Surlyn inclusion can be regarded as a single dispersed phase. Here, the following log-additivity rule is used to calculate η^* [18,19]:

$$\log\eta_c^* = \phi_{PP}\log\eta_{PP}^* + \phi_{inclu}\log\eta_{inclu}^* \quad (3)$$

or

$$\log\eta_c^* = \phi_{PP}\log\eta_{PP}^* + (1-\phi_{PP})\log\eta_{inclu}^* \quad (4)$$

where Φ_{PP} and Φ_{inclu} are the volume fraction, η_{PP}^* and η_{inclu}^* are the complex viscosities of PP and dispersed inclusions, respectively. Note that η_{inclu}^* is obtained from binary Surlyn/OMMT hybrids prepared at the same condition, in which the same Surlyn/OMMT ratio as PP20CN hybrids is maintained. The density of PP, Surlyn, and C20A was adopted to be 0.91, 0.96, and 1.77 g/cm^3, respectively. The calculated and experimental results for PP20 and PP20CN hybrid

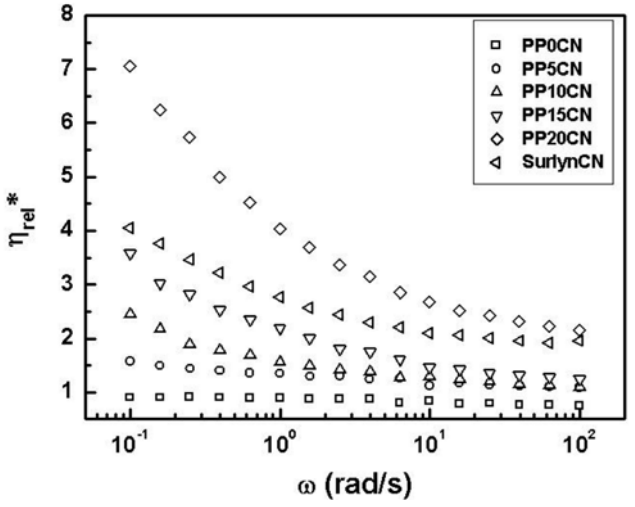

Fig. 7. Relative complex viscosity (η_{rel}^*) of PP-Surlyn-OMMT hybrids at 180 °C.

are shown in Fig. 8. The calculated data of PP20 based on log-additivity rule are a little higher than the measured data in Fig. 8(a).

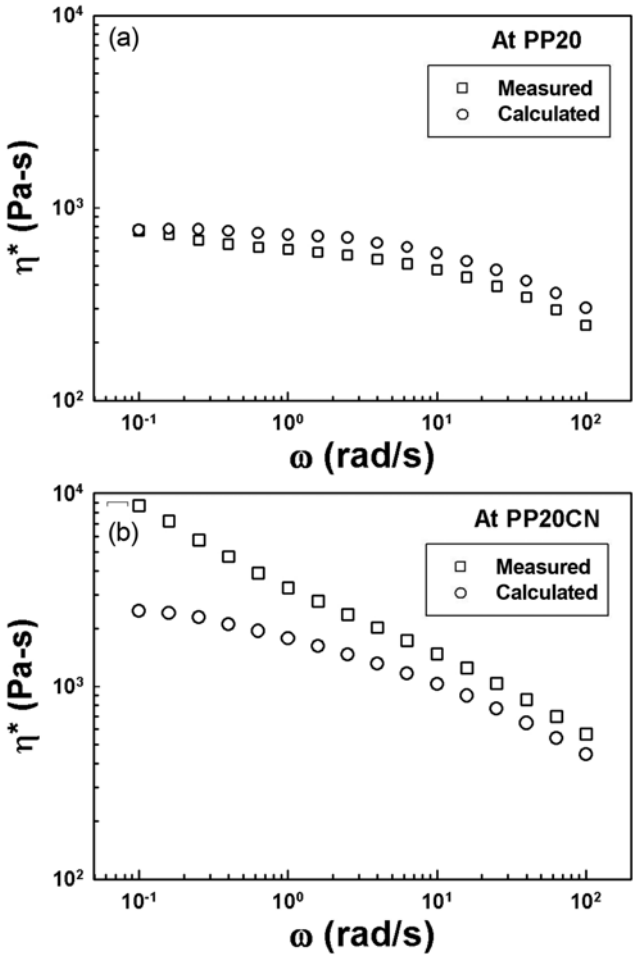

Fig. 8. Theoretical and experimental curves of complex viscosity (η_c^*) of PP20 and PP20CN hybrid.

This result implies that the interface interaction between PP and Surlyn is weak. On the other hand, over the whole frequency range investigated, the experimental data of the PP20CN hybrid are always higher than predicted in Fig. 8(b), which in turn supports the above assumption.

4. Crystallization

The influence of added organoclay on the bulk crystallization of PP matrix in PP/Surlyn/OMMT hybrid was investigated using DSC. At the same time, corresponding PP/Surlyn samples were measured as a comparison. The cooling and subsequent heating curves for PP/Surlyn and PP/Surlyn/OMMT are shown in Fig. 9. Each curve was shifted vertically along the Y-axis for clarity. The broad endothermic peak at approximately 90 °C in the samples containing Surlyn arises from the melting of the ionomer. The calculated crystallization characteristics of PP matrix are summarized in Table 2. As expected, PPCN exhibits the highest crystallization peak temperature (5.4°C higher than pure PP control) and crystallinity due to the heterogeneous nucleation of clay tactoids. In case of PP/Surlyn blends, a similar T_c increase of PP matrix is clearly observed as well, although a slightly decrease in T_c^{peak} is observed as a function of Surlyn concentration. This could result from ionic aggregates of Surlyn domains in the binary blends. Small-angle X-ray scattering experiment showed that the ionic aggregates within ionomer can persist

Table 2. Crystallization data for PP in PP/Surlyn and PP/Surlyn/OMMT

Surlyn concentration (wt%)	Code name	T_c^{onset} (°C)	T_c^{peak} (°C)	Crystallinity χ(%)
PP/Surlyn/OMMT				
0	PP0CN	124.7	116.2	48.41
5	PP5CN	122.9	111.4	44.88
10	PP10CN	122.7	110.9	43.59
15	PP15CN	122.5	111.0	43.41
20	PP20CN	122.5	110.2	43.65
PP/Surlyn				
0	PP	121.2	110.8	44.80
5	PP5	124.9	115.8	46.98
10	PP10	124.3	114.9	45.41
15	PP15	124.0	114.0	44.48
20	PP20	124.7	113.3	45.09

Cycle: 50 °C----230 °C (5 min)-----50 °C------230 °C at the heating/cooling rate of 10 °C/min; T_c^{onset} is the temperature at which the thermogram departs from the baseline at the beginning of the exotherm

in the molten state up to 300 °C [20-22], which is much higher than the melting temperature of PP. In practice, Surlyn has been widely used as an aiding agent for PET crystallization.

On the other hand, the increased T_c fails to be observed in the ternary hybrids. Compared to the data of both PPCN and PP/Surlyn, there seemingly exists a synergistic effect between Surlyn and clay in suppressing their accelerating crystallization on PP matrix. It is well-documented that the reason for more improved exfoliation of organoclay in ionomers with respect to non-ionic polymeric analogues mainly attributes to the interaction of the ionic groups with the aluminosilicate surface of the clay [23-29]. Thus, it is reasonable to assume that in our ternary hybrids, there exists a strong charge interaction between clay platelets and ionic aggregates in Surlyn phase, which could weaken nucleating effect of ionic aggregates on PP matrix. Furthermore, the clay platelets localized at the interface prevent the contact of Surlyn domains from PP matrix during crystallization. The crystallization kinetics of polymers is determined not only by nucleation but also by growth rate of spherulites. As for the failure of clay particles localized at the interface to induce crystallization of PP, the authors attribute it to their fine dispersion, which hinders the mobility of polymer chains, resulting in a decrease in the crystallization growth rate despite the enhanced nucleating activity of PP matrix. The former effect could counteract the nucleating contribution of clays. Recently, some researchers reported that the improved dispersion of clay does not contribute to an increase in T_c of PP matrix in PP-clay nanocomposites, but others led to an opposite trend [30-35]. Svoboda et al. observed the acceleration of isothermal DSC crystallization only in PP/PP-MA/OMMT systems containing clay tactoids, while no OMMT nucleation in the systems with well dispersed clay platelets was observed [30]. Perrin-Sarazin et al. found that PP/OMMT hybrid showed the highest crystallization rate among the materials tested, while for PP/PP-g-MA/OMMT samples the crystallization occurred at much lower crystallization rates and at only slightly above that of pure PP [31]. They argued that PP-clay interface played an important role in the crystallization

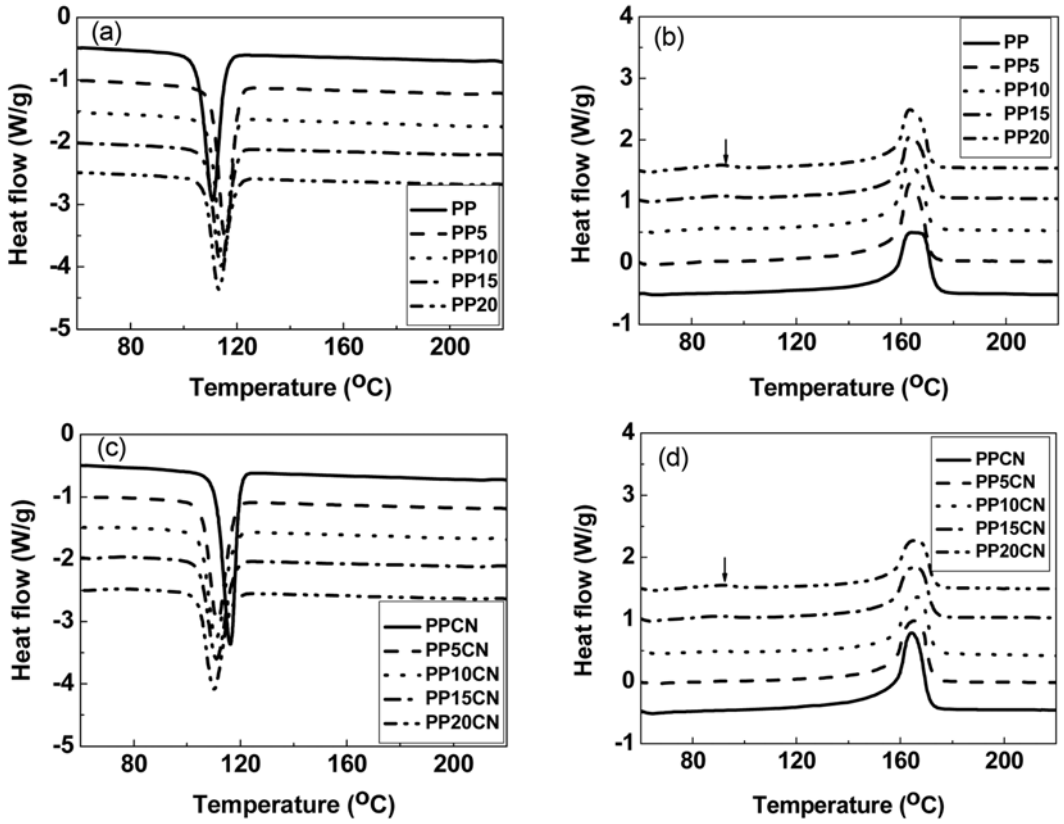

Fig. 9. DSC cooling and second heating thermograms for PP/Surlyn (a, b) and PP/Surlyn/OMMT (c, d) respectively.

behavior, with specific PP-clay interaction involving MA groups of the coupling agent that limited the nucleating effect of the clay particles. Kim and coworkers studied the isothermal crystallization of maleic anhydride grafted polypropylene-based nanocomposites, and the same result was found [35]. They explained this retardation of PP crystallization due to the presence of well-dispersed exfoliated silicates as a diffusion barrier for crystallization. Similar results were obtained by other research groups [33-35].

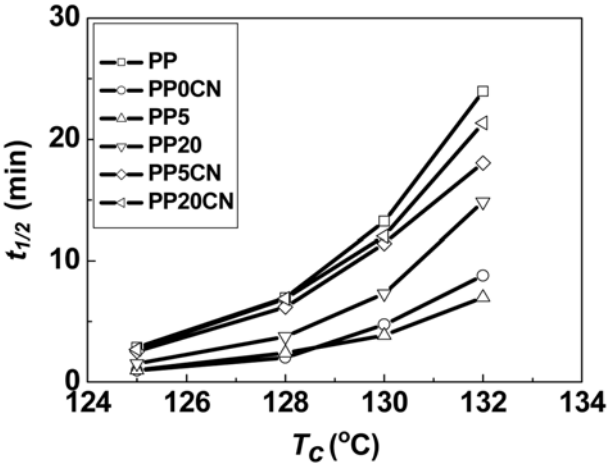

Fig. 10. The reciprocal of half-time of crystallization ($\tau_{1/2}$) versus crystallization temperature (T_c) during isothermal crystallization.

In order to compare the overall crystallization rate of these samples, four different temperatures (T_c=125, 128, 130, and 132 °C) were chosen, respectively, for the analysis of isothermal crystallization kinetics. Half-time of crystallization ($t_{1/2}$) is defined by the time at which half of the relative crystallinity is reached. Fig. 10 shows the dependence of $t_{1/2}$ on crystallization temperature. The smaller $t_{1/2}$ value means faster crystallization rate, and thus one can obtain that the crystallization rate for these samples ranks as PPCN≈PP5>PP20> PP5CN≈PP20CN≈PP. The order is related with that of crystallinity in Table 2. The slower crystallization rate is, the higher crystallinity is.

Based on the above discussion, such a synergistic role between Surlyn and OMMT during PP crystallization could be generalized as follows: first, the addition of Surlyn greatly improves the dispersion of C20A, and some of silicate layers selectively locate at the interphase. On the other hand, the well-dispersed silicates at the interface not only limit their own nucleation activity, but also suppress nucleating activity of Surlyn on PP matrix. The microstructural difference is schematically depicted in Fig. 11. The specific migration mechanism of clay platelets toward interface during compounding is still under investigation and we will report it in the future. Additionally, the melting peak temperature of PP matrix slightly differs from PP control. This result indicates that the addition of either Surlyn or OMMT fails to significantly alter the melting behavior of PP phase.

5. Mechanical Properties

Fig. 12 shows tensile data of PP/Surlyn/OMMT hybrids, together with corresponding PP/PP-g-MA/OMMT as a comparison. Rela-

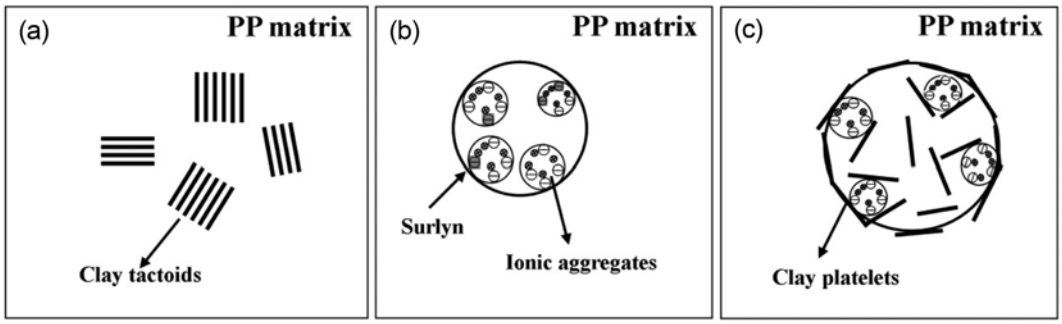

Fig. 11. Schematic diagram of the dispersed morphology in the blend and hybrids: (a) PP/OMMT; (b) PP/Surlyn; (c) PP/Surlyn/OMMT.

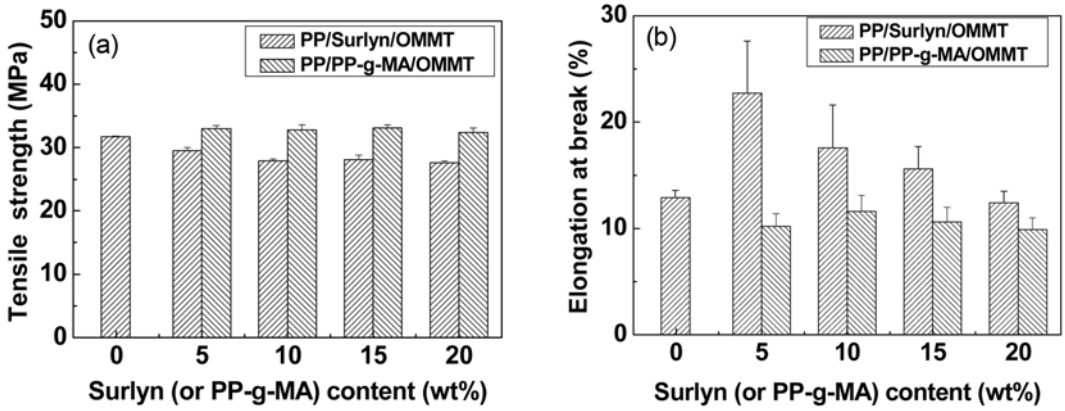

Fig. 12. Tensile properties for PP-based clay hybrids: (a) tensile strength; (b) elongation at break.

tive to pure PP, PP/OMMT without Surlyn (i.e., PP0CN) exhibits a decrease in both tensile yield strength and elongation at break. This could be attributed to a poor dispersion of clay in PP matrix. However, the situation is different in PP/Surlyn/OMMT systems. The tensile strength is slightly decreased for about 7% with respect to PP0CN when 5 wt% Surlyn is added. With further increase in ionomer concentration, the strength does not decrease significantly and remains at an acceptable level as a whole. However, the addition of 5 wt% Surlyn leads to a substantial improvement in elongation at break (approximately 176% compared to PP0CN). With further increasing Surlyn concentration in the ternary hybrids, a progressive decrease in fracture strain is observed. It is different from almost unchanging thermal property in Fig. 9(b). But the elongation of Surlyn system is still higher than that of PP-g-MA system. In rubber or elastomer-toughened thermoplastics, toughening depends not only on rubber content and size, but also on rubber modulus and interfacial adhesion. It is well established that shear yielding of polymer matrix induced by microvoids of rubber domain is the main energy-dissipating mechanism in the deformation process [36]. In our case, no remarkable change in the size of ionomer phase was observed with increasing Surlyn content based on TEM images. The reduced fracture strain with Surlyn addition is likely to result from the reduced elasticity of Surlyn due to the improved exfoliation of clay silicates within the ionomer phase [1,2]. As a result, the ability of the dispersed ionomer particles to form cavitation under uniaxial tensile stress is decreased. A similar conclusion was also drawn by Yu et al., who studied the effect of blending sequence on the microstructure of nylon66/organoclay/SEBS-g-MA ternary nanocomposites [37,38]. They found that the presence of organoclay in SEBS-g-MA phase reduced the ability to form cavitation, resulting in reduced toughening efficiency. Another possible reason is attributed to the fact that the interfacial bonding between Surlyn and PP matrix is not sufficient enough to prevent debonding of Surlyn domains prior to the induced yielding of PP matrix.

The aforementioned TEM pictures demonstrate that some of silicate layers are localized at the phase boundary between PP and Surlyn. To evaluate the influence of such a selective localization of clays on interfacial adhesion between PP and Surlyn, we further analyzed yield strength data with different model equations. Because clays are selectively localized within Surlyn domain, the Surlyn particle containing OMMT can be regarded as a dispersed inclusion in PP matrix. In the ideal case, the yield strength, σ_{yb}, of a particulate system, in which the dispersed particles do not yield and have a good adhesion to the matrix, is approximately equal to that of the matrix σ_{ym}. In practice, however, σ_{yb} usually tends to reduce with increasing volume fraction of the dispersed phase. As for the variation of tensile yield stress with immiscible blend composition, Nielsen proposed the following simple equation [39]:

$$\sigma_{yb}=\sigma_{ym}(1-\phi_d^{2/3}) \tag{5}$$

where σ_{yb} and σ_{ym} are the yield stresses of the blend and matrix, respectively, ϕ_d the volume fraction of the inclusion. This equation indicates that the yield strength of incompatible blends decreases with increasing volume fraction of the dispersed phase. Nicolais and Narkis' modified Eq. (3) for composite systems lacking interfacial adhesion by changing the multiplication factor for $\phi^{2/3}$ from 1

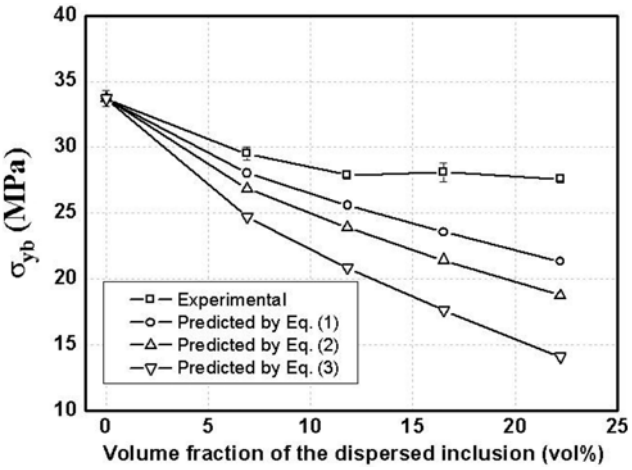

Fig. 13. Experimental and theoretic values of σ_{yb} as a function of volume fraction of the dispersed inclusion (including Surlyn and OMMT) for the PP/Surlyn/OMMT hybrids.

to 1.21 as follows [40]:

$$\sigma_{yb}=\sigma_{ym}(1-1.21\phi_d^{2/3}) \quad (6)$$

In the extreme case of no adhesion between the matrix and dispersed phase, the yield stress of a composite can be predicted as follows [41,42]:

$$\sigma_{yb}=\sigma_{ym}\left[1-\frac{(\phi_d)^{2/3}}{\phi_{max}}\right] \quad (7)$$

where the ϕ_{max} is the maximum packing fraction of the dispersed phase (here taken ϕ_{max}=0.63 for random close-packing of monodisperse spheres [43]). Inserting the experimental value of σ_{ym}=33.7 MPa for PP matrix and ϕ_d into the above equations, we can calculate σ_{yb} and the results are shown in Fig. 13. The predictions are based on the measured yield stress of pure PP. All the experimental values for ternary silicate hybrids are higher than the predictions. This result suggests that the selective localization of silicate layers at the interface is indeed beneficial to the partial improvement in interfacial adhesion between PP and Surlyn, which agrees well with the previous SEM observation.

CONCLUSIONS

Surlyn ionomer was added (up to 20 wt%) into PP/C20A hybrids, and the properties and morphology of the resulting hybrids were investigated by XRD, SEM, TEM, rheological characterization, DSC and tensile test. Morphological observation revealed that the addition of ionomer significantly enhanced the dispersion of clays. Apart from the localization inside the dispersed Surlyn domain, clay platelets were also localized at the interface between PP and Surlyn. The selective localization in turn improved the interface adhesion between the two phases, as evidenced by SEM pictures. Unlike the corresponding PP/Surlyn binary blends, the viscoelastic properties of the ternary hybrids exhibited a remarkable increase upon the addition of the ionomer, which could be attributed to the increased exfoliation of clays and interfacial contribution caused by silicate layers at the interface. Interestingly, the nucleating effect of both Surlyn and clay on PP matrix in the PP/Surlyn/OMMT hybrids was suppressed due to the synergistic action between them. When 5 wt% Surlyn was added, the elongation at break of PP-OMMT hybrid was remarkably increased in comparison to the corresponding PP0CN and PP/PP-g-MA/OMMT. On the other hand, further addition of the ionomer resulted in a gradual decrease, which could arise from the reduced ability of Surlyn domains to initiate cavitation due to clay exfoliation. At the same time, the yield strength of the hybrids remained at a satisfactory level. By comparing the predicted values of yield strength with experiments, the clay layers at the interface were found to act as a positive role of improved interfacial adhesion between immiscible PP and Surlyn, which is coincident with SEM micrographs.

ACKNOWLEDGMENTS

This work was supported by the National Research Foundation of Korea (NRF) grant funded by the Korea government (MEST) (20090085024).

REFERENCES

1. R. K. Shah, D. L. Hunter and D. R. Paul, *Polymer*, **46**, 2646 (2005).
2. R. K. Shah and D. R. Paul, *Macromolecules*, **39**, 3327 (2006).
3. R. K. Shah, R. K. Krishnaswamy, S. Takahashi and D. R. Paul, *Polymer*, **47**, 6187 (2006).
4. S. Sanchez-Valdes, M. L. Lopez-Quintanilla, E. Ramirez-Vargas, F. J. Medellin-Rodriguez and J. M. Gutierrez-Rodriguez, *Macromol. Mater. Eng.*, **291**, 128 (2006).
5. J. W. Lim, A. Hassan, A. R. Rahmat and M. U. Wahit, *J. Appl. Polym. Sci.*, **99**, 3441 (2006).
6. J. K. Mishra, K. J. Hwang and C. S. Ha, *Polymer*, **46**, 1995 (2005).
7. H. S. Lee, P. D. Fasulo, W. R. Rodger and D. R. Paul, *Polymer*, **46**, 11673 (2005).
8. H. S. Lee, P. D. Fasulo, W. R. Rodger and D. R. Paul, *Polymer*, **46**, 3528 (2005).
9. J. W. Lim, A. Hassan, A. R. Rahmat and M. U. Wahit, *Polym. Inter.*, **55**, 204 (2006).
10. S. C. Tjong, S. P. Bao and G. D. Liang, *J. Polym. Sci. Part B: Polym. Phys.*, **43**, 3112 (2005).
11. The data were provided by the supplier.
12. J. M. Li, M.-T. Ton-That and S.-J. Tsai, *Polym. Eng. Sci.*, **46**, 1060 (2006).
13. M. Si, T. Araki, H. Ade, A. L. D. Kilcoyne, R. Fisher, J. C. Sokolov and M. H. Rafailovich, *Macromolecules*, **39**, 4793 (2006).
14. S. S. Ray, S. Pouliot, M. Bousmina and L. A. Utracki, *Polymer*, **45**, 8403 (2004).
15. J. S. Hong, H. Namkung, K. H. Ahn, S. J. Lee and C. Kim, *Polymer*, **47**, 3967 (2006).
16. Y. Wang, F. B. Chen, K. C. Wu and J. C. Wang, *Polym. Eng. Sci.*, **46**, 289 (2006).
17. C. Koning, M. V. Duin, C. Pagnoulle and R. Jerome, *Prog. Polym. Sci.*, **23**, 707 (1998).
18. L. A. Utracki and B. Schlund, *Polym. Eng. Sci.*, **27**, 1512 (1987).
19. N. S. Rao and G. Schumacher, in *Design formulas for plastics engineers*, 2nd ed., Hanser, Munich, 1 (2004).
20. F. C. Wilson, R. Longworth and D. J. Vaughan, *Polym. Prepr.*, **9**,

505 (1968).
21. D. J. Yarusso and S. L. Cooper, *Polymer*, **26**, 371 (1985).
22. R. A. Register, X. H. Yu and S. L. Cooper, *Polym. Bull.*, **22**, 565 (1989).
23. G. D. Barber, B. H. Calhoun and R. B. Moore, *Polymer*, **46**, 6706 (2005).
24. B. J. Chisholm, R. B. Moore, G. Barber, F. Khouri, A. Hempstead, M. Larson, E. Olson, J. Kelley, G. Balch and J. Caraher, *Macromolecules*, **35**, 5508 (2002).
25. J. A. Lee, M. Kontopoulou and J. S. Parrent, *Polymer*, **46**, 5040 (2005).
26. J. S. Parent, A. Liskova and R. Resendes, *Polymer*, **45**, 8091 (2004).
27. N. N. Bhiwankar and R. A. Weiss, *Polymer*, **46**, 7246 (2005).
28. N. N. Bhiwankar and R. A. Weiss, *Polymer*, **47**, 6684 (2006).
29. P. Govindaiah, S. R. Mallikarjuna and C. Ramesh, *Macromolecules*, **39**, 7199 (2006).
30. P. Svoboda, C. C. Zhen, H. Wang, L. J. Lee and D. L. Tomasko, *J. Appl. Polym. Sci.*, **85**, 1562 (2002).
31. F. Perrin-Sarazin, M. T. Ton-That, M. N. Bureau and J. Denault, *Polymer*, **46**, 11624 (2005).
32. B. Kim, S. H. Lee, D. Lee, B. Ha, J. Park and K. Char, *Ind. Eng. Chem. Res.*, **43**, 6082 (2004).
33. A. Somwang Thanaroj, E. C. Lee and M. J. Solomon, *Macromolecules*, **36**, 2333 (2003).
34. R. Nowacki, B. Monasse, E. Piorkowska, A. Galeski and J. M. Haudin, *Polymer*, **45**, 4877 (2004).
35. F. C. Chiu, S. M. Lai, J. W. Chen and P. H. Chu, *J. Polym. Sci. Part B: Polym. Phys.*, **42**, 4139 (2004).
36. G. M. Kim and G. H. Michler, *Polymer*, **39**, 5699 (1998).
37. A. Dasari, Z. Z. Yu and Y. W. Mai, *Polymer*, **46**, 5986 (2005).
38. A. Dasari, Z. Z. Yu, M. Yang, Q. X. Zhang, X. L. Xie and Y. W. Mai, *Comp. Sci. Technol.*, **66**, 3097 (2006).
39. L. E. Nielsen. *J. Appl. Polym. Sci.*, **10**, 97 (1966).
40. L. Nicolais and M. Narkis, *Polym. Eng. Sci.*, **11**, 194 (1971).
41. L. Nicolais and M. Narkis, *Polym. Eng. Sci.*, **10**, 97 (1971).
42. J. Kolarik, G. L. Agrawal, Z. Krulis and J. Kovar, *Polym. Compos.*, **7**, 463 (1986).
43. L. E. Nielsen and R. F. Landel, in *Mechanical properties of polymers and composites*, Marcel Dekker, New York, 378 (1994).